Radiation of Finite-amplitude Waves from a Baffled Pipe

K. Joshua Bodon

A senior thesis submitted to the faculty of
Brigham Young University
in partial fulfillment of the requirements for the degree of

Bachelor of Science

Kent Gee, Derek Thomas, Advisors

Department of Physics and Astronomy

Brigham Young University

August 2013

ABSTRACT

Radiation of Finite-amplitude Waves from a Baffled Pipe

K. Joshua Bodon

Department of Physics and Astronomy

Bachelor of Science

The radiation of finite-amplitude waves from the open end of a baffled, circular pipe is considered as a direct continuation of work begun by Kuhn, Blackstock, and Wright more than three decades ago [Kuhn et al., J. Acoust. Soc. Am. 63, S1, S84 (1978)]. Band-limited Gaussian noise, as well as 1 kHz, 1.5 kHz, and 2kHz sinusoidal pulses, with initial peak pressure amplitudes ranging from 0.5 – 1.2 kPa, have been propagated down a 6.1 m pipe, whose open end (5.1 cm inner diameter) has been placed off-center in a large rectangular baffle. As the steepened or shock-like waves exit the pipe, the measured waveforms are comprised of sharp impulses that are delta function-like in nature, particularly on axis. Although linear piston theory predicts similar waveform shapes, there is also evidence that nonlinear propagation of these impulses, which can exceed peak pressure amplitudes of 1.5 kPa near the pipe opening, is occurring.

Contents

List of Figures

Chapter 1

Introduction

1.1 Previous Work Done

Propagation of finite-amplitude acoustic waves in an open-ended pipe can result in radiated waveforms that contain large positive impulses, particularly on axis. This phenomenon has been observed in several applications including waveforms exiting trombones and engine noise entering a muffler chamber. Both Hirschberg [1] and Thompson and Strong [2] recorded sharp impulses exiting the horn of a trombone when played at high levels. While the work done by Hirschberg [1] resulted in far more dramatic impulses at high amplitude than those of Thompson and Strong [2] both show a steep increasing slope followed by a large negative slope in the positive waveform.

Sekine [3] recorded pressure waveforms inside of exhaust pipes and similarly recorded peaks just inside the muffler similar to those observed by Thompson and Strong. Although Sekine, Thompson and Strong, and Hirschberg were not specifically studying radiation of high amplitude waveforms from a finite aperture both have shown that nonlinear wave steepening occurs inside trombones when played at fortissimo levels as well as in exhaust pipes, and that sharp, delta function-like peaks occur outside a finite

aperture [1] [2] [3]. Others have made a specific study of these radiation patterns. For example, Kim and Setoguchi [4] demonstrated this behavior in their study of unsteady weak shocks exiting a baffled pipe, and Nakamura and Takeuchi [5] performed a frequency-domain analysis of N-wave radiation from an unbaffled pipe. Although both of these examples involved transient radiation, the phenomenon extends to continuous waves. Similar waveforms were also documented by Gee *et al.* [6] when the U. S. Army Research Laboratory's Mobile Acoustic Source was driven with initially sinusoidal waves at high amplitudes.

In the late 1970's, Blackstock, Wright, and Kuhn [7] [8] investigated continuous-wave, finite-amplitude radiation from the end of a flanged pipe. Their experimental apparatus consisted of a 3 m long pipe with a 5.1 cm inner diameter with a flanged opening. They drove the pipe using 8 kHz sinusoidal pulses at 138 dB re 20 μPa while pressure measurements were made at various locations outside of the pipe. An example of a single cycle is shown in Fig. 1.1 and is representative of the highly asymmetric pulses that were measured. The authors considered the nonlinear steepening inside the pipe but compared their results with linear piston theory outside. The work done in the current paper represents a continuation and extension of work by Blackstock *et al* [8] by analyzing the production and propagation of high-amplitude, continuous waveforms from the end of a baffled pipe.

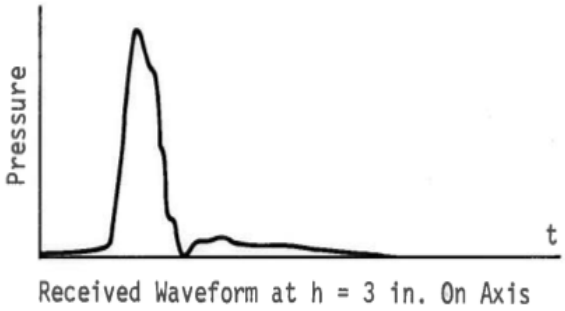

Figure 1.1 Measured Waveform from Blackstock *et al.*

The experimental setup considered in this work uses a longer pipe driven with a higher amplitudes and a larger baffle than Blackstock. Furthermore, the excitation frequency has been limited to below the first cross mode of the pipe, which will facilitate comparison with piston theory. Results discussed in this paper are limited to 1 kHz sinusoidal pulses with initial peak sound pressure levels of 155 dB re 20 μPa.

1.2 Background Information

In order to understand why the waveform transforms from a shockwave shape to an impulse like shape upon exiting the pipe it is of some use to examine basic shock formation theory necessary to describe the acoustic propagation inside the pipe. As a sinusoidal waveform is propagated down any length of tube its shape begins to distort. The positive peaks appear to shift backwards as the troughs shift forwards in the waveform, creating a slope approaching infinity between the maximum and minimum pressures. This waveform as shown in Figure 1.2 is commonly referred to as a shock wave, sawtooth wave, or a N-wave and is caused in part due to high amplitudes affecting

the sound speed. In addition to the distortion of the waves shape an amplitude loss also occurs.

The magnitude of the nonlinear steepening can be related numerically through the shock formation distance, which can be expressed as $\bar{x} = \frac{\rho_0 c^3}{\beta\ \omega\ p_0}$ (eq. 1.1), with β a constant and sound speed c. Shock formation distance $\bar{x}$ is heavily dependent on several factors including angular frequency ω, and initial pressure of the wave p_0. As outlined in eq. 1.1, if either of pressure or frequency are increased the distance it takes to create a stronger shock-wave is reduced. The dimensionless shock formation distance is commonly referred to as $\sigma = \frac{x}{\bar{x}}$ (eq. 1.2.), and describes how developed a shock wave will be at the end of a tube by relating a distance relative to the shock formation distance $\bar{x}$.

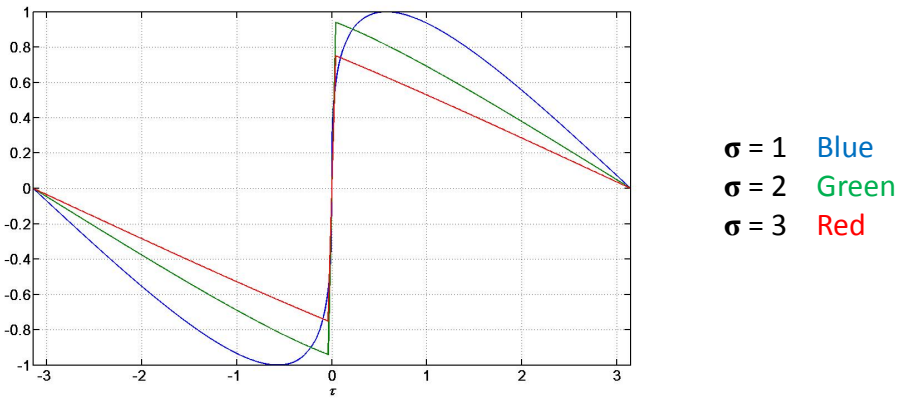

Figure 1.2 Examples of distortion that occurs for σ values of 1 (Blue), 2 (Green) and 3 (Red)

$$\bar{x} = \frac{\rho_0 c^3}{\beta\ \omega\ p_0} \tag{1.1}$$

$$\sigma = \frac{x}{\bar{x}} \tag{1.2}$$

Chapter 2

Setup and Experimental Procedure

Like the original experiments by Blackstock *et al.,*[8] a 5.1 cm inner diameter pipe was used, which limits the initial excitation bandwidth to below 4 kHz to prevent cross modes. A BMS 4592 compression driver with a 5.1 cm throat diameter, 1300 W peak power capability, and a nominal frequency response between 300 – 7000 Hz was used in conjunction with an 1100 W Crown XS1200 Power Amplifier. Signal output and acquisition was carried out using National Instruments USB-6259 device with a 1MHz aggregate sampling rate input and 2.8 MH sampling rate output. Pressure data were obtained using 3.18 mm 40DD GRAS microphones. Three microphones were placed along the pipe at distances of 5.7, 310.5, and 605.4 cm, from the driver, as shown in Fig. 2.1.

The microphones were mounted without grid caps so the diaphragms were flush with the inner wall surface of the pipe. A fourth microphone was moved to various positions at the height of the pipe centerline in order to measure the waveforms radiated from the end of the pipe. The exit of the pipe was flush mounted into a 1.23 m by 1.24 m baffle made from medium density fiberboard. The pipe axis was located 9.5 cm horizontally

and 8.2 cm vertically from the center of the baffle in order to reduce waves scattered by the edges of the baffle from arriving coherently at the on-axis microphone locations. As shown in Fig. 2.2, the baffle was placed in an 8.71 m x 5.66 m x 5.74 m anechoic chamber with the driver side of the pipe running out the door. During all measurements the anechoic doors to the chamber were closed around the pipe to limit reflections from the hallway.

To create the radiation of these sharp impulses, a steepened or shock-like wave must be generated in the pipe. However, an initial sawtooth response cannot be used because the higher harmonics would likely generate cross modes within the pipe. Thus, to produce a shock-like response at the end of the tube, significant nonlinear steepening must occur from an initial signal with dominant frequencies below the ~4 kHz cutoff frequency of the first cross mode. This ensures a planar wavefront across the face of the fluid piston at the pipe opening. The pipe length is a key factor in this process because it determines the number of shock formation distances the wave travels before exiting the pipe.

The calculated shock formation distance for the parameters used by Blackstock *et al.* [7] (an initial 8 kHz sinusoid at138 dB re 20 μPa in a 3 m pipe) reveals that the waveforms had not yet reached one shock formation distance upon exiting the pipe. This relatively weak nonlinear steepening differs considerably from the unsteady shock experiment of Kim and Setoguchi [4]. For our experiment, space constraints limited our pipe to 6.1 m, which meant for our 1 kHz, 155 dB re 20 μPa waveform, the tube was approximately two shock formation distances in length. This condition results in a waveform approaching a sawtooth-like condition at the end of the pipe [9], in the absence

of the interior reflection occurring from the open end of the pipe. In order to measure the initial waveform near the driver without the influence of reflections, sinusoidal pulses of approximately 35 ms in length were used.

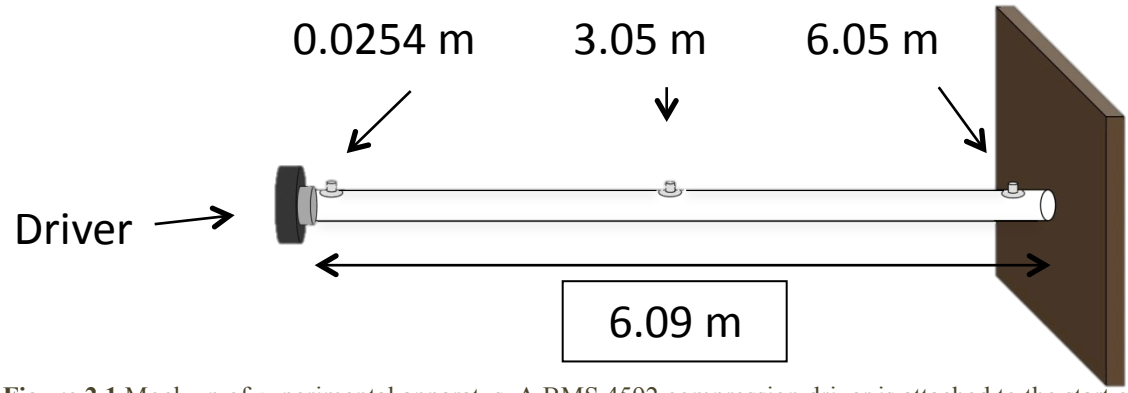

Figure 2.1 Mock up of experimental apparatus. A BMS 4592 compression driver is attached to the start of the pipe and an 8.71 m x 5.66 m x 5.74 m baffle is flush mounted to the end. Microphones were placed at 0.0254, 3.05, and 6.05 m along the 6.09 m pipe.

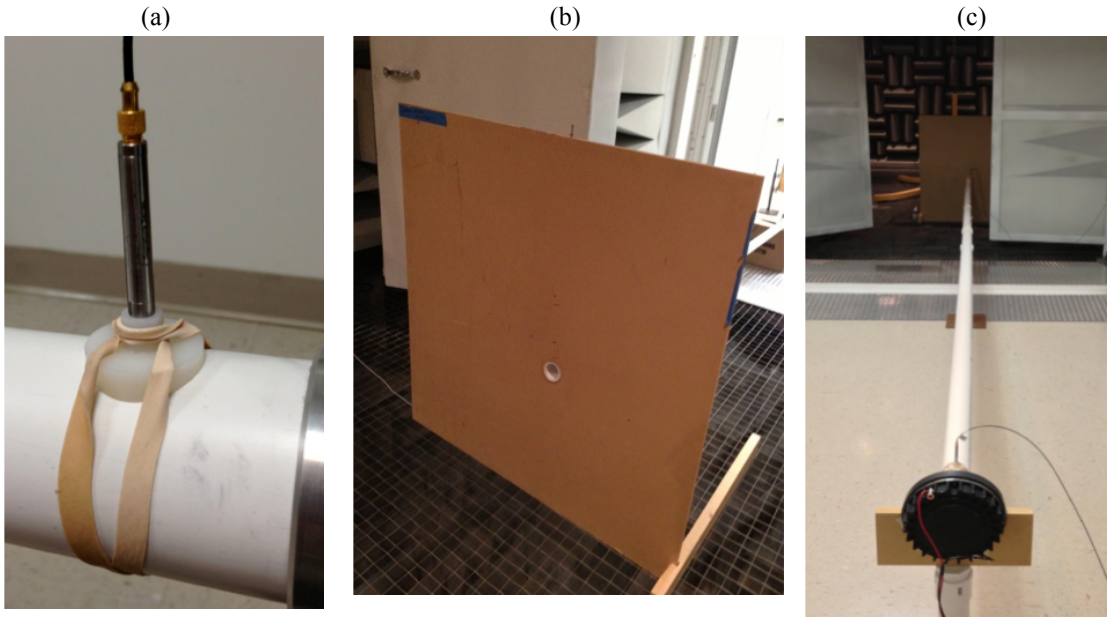

Figure 2.2 Photographs of setup. (a) microphone mounted in pipe, (b) baffle flush mounted to end of pipe, (c) pipe terminating in anechoic chamber.

Chapter 3

Discussion of Results

Pressure data were collected both inside and outside of the pipe in a variety of locations. In the following sections a discussion will be made in an effort to characterize the effects that different measurement locations, initial frequencies, and initial amplitudes have on a radiated waveform.

3.0 Geometries

For the convenience of the reader the following geometries will hold for the remainder of this thesis (Fig. 3.1, 3.2). Additionally, except where noted, each initial signal should be considered a 1 kHz sinusoidal pulse.

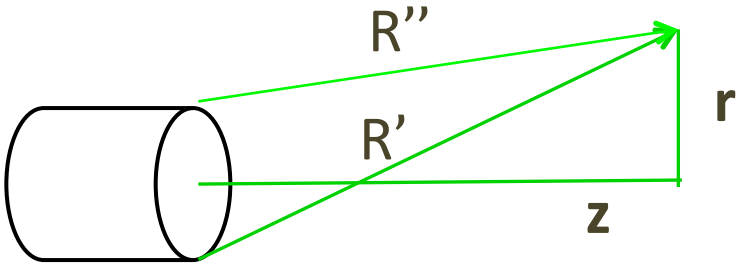

Figure 3.1 Distance Labels: z represents on-axis distance from the center of the pipe, r is the off-axis distance from the center of the pipe, R' represents the distance from the farthest edge of the pipe to measurement location, R'' represents the distance from the closest edge of the pipe to the measurement location.

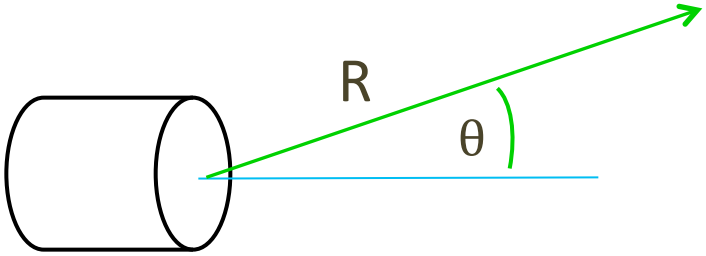

Figure 3.2 Geometry: R representing the distance from the center of the pipe at the aperture to the measurement location, θ represents the angle from the axis of the pipe at the measurement location.

3.1 Inside the Pipe

Measured results provide evidence of nonlinear effects occurring inside of the pipe. The data displayed in Fig. 3.3 clearly demonstrate steepening inside of the pipe. Figures 3.3 (a-c) show steepening of the sinusoid into a shock-like waveform as the sinusoid propagates from 5.7 to 310.5 and then to 605.4 cm, respectively. The data shown in Fig. 3.3 (d) are from a microphone placed on axis, at R=3.8 cm. Figure 3.3 (a) demonstrates

that the pressure at the driver is sinusoidal with amplitude of about 1.2 kPa, while Fig 3.3 (b) shows a slight reduction in amplitude from the original signal and a definite steepening towards shock formation approximately halfway down the pipe. At the microphone closest to the pipe's aperture the waveform as displayed in Fig. 3.3 (c), has become distorted with an appreciable increase in amplitude due to the reflection from the boundary at the end of the pipe. As described, short pulses of 35 ms were propagated in order to reduce interference from incident and reflecting waves in most of the pipe, however the third microphone was placed only 4 cm from the piston face. This is equivalent to approximately 0.2 ms at a 343 m/s sound speed, less than the period of a 1 kHz signal, creating unavoidable interference at this location. Even as the wave becomes more asymmetric due to these reflections, shock wave characteristics are still noticeable. Figure 3.3 (d) depicts sharp narrow pressure peaks produced on-axis 3.8 cm outside of the tube, similar to those noted in previous studies, but higher in amplitude than the continuous wave examples seen in Refs. 4, 5, and 7.

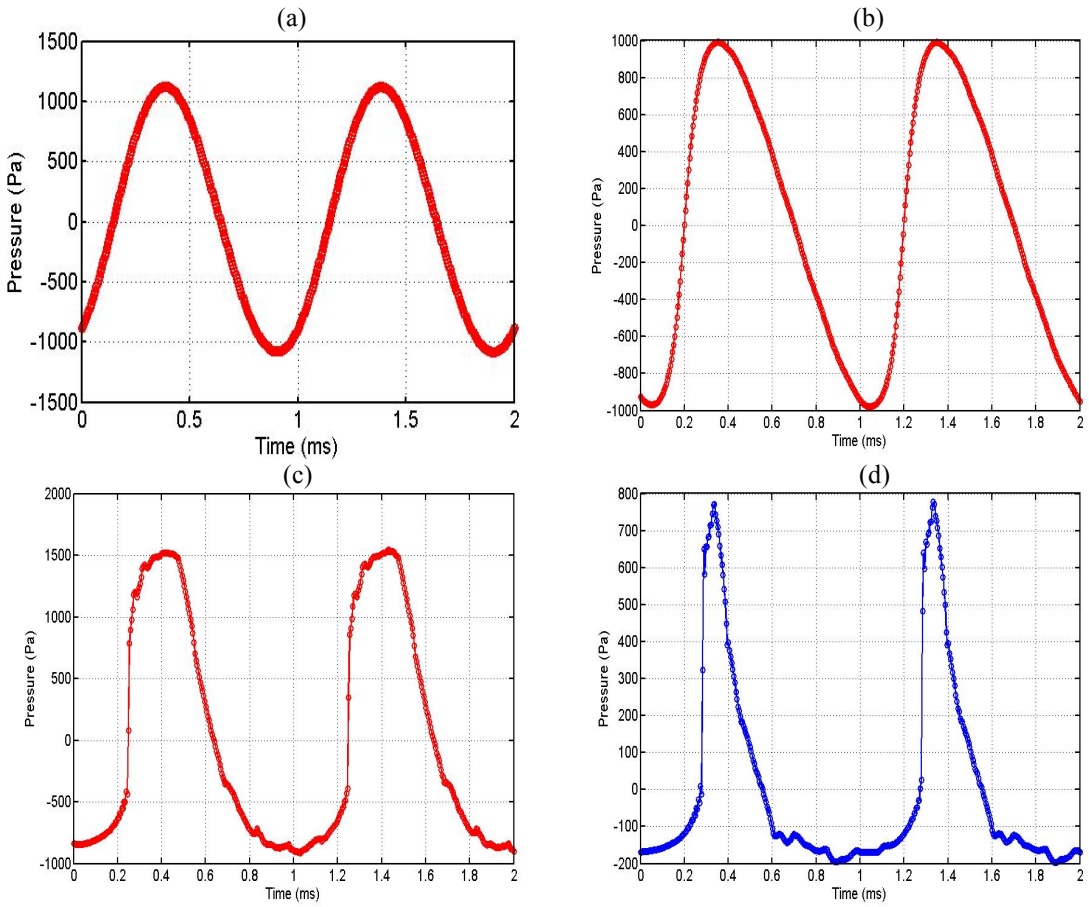

Figure 3.3 Pressure waveforms for a 1 kHz sinusoid initial pulse inside tube at (a) 2.54 cm, (b) 305 cm, (c) 605 cm. (d) pressure waveform outside the tube on-axis 3.8 cm from the baffle.

The waveform's shape outside the pipe can be qualitatively explained by considering the linearized momentum (Euler's) equation in one dimension (x), which can be written as $\rho_0 \dot{u} = -p_x$. Under this linear approximation, the particle acceleration, $\dot{u}$, and pressure gradient, p_x, are proportional to one another via the ambient density, ρ_0. The rapid spatial change in the pressure due to the acoustic shocks produces large accelerations at the end of the pipe. From linear piston theory, the far-field, on-axis pressure is proportional to the particle acceleration at the fluid piston face [10]. Far-field being defined as a distance greater than the Rayleigh distance $R_0 = \frac{ka^2}{2}$ (eq. 3.1) from

the pipe's face, where k is the wavenumber and a is defined to be the pipe radius [10]. Although the Rayleigh distance for the piston varies between 0.59 cm and 59 cm over a frequency range of 1 – 100 kHz (Table 1), such that the measurement in Fig. 3.3 (d) is in the near field at the highest frequencies measured, the derivative of the pressure in Fig. 3.3 (c) can still be matched in a qualitative sense to the radiated shape in Fig. 3.3 (d). This positive impulse is similar to those seen by both Kim and Setoguchi [4] and Hirschberg *et al.* [1] but appears more shock-like than those measured previously by Blackstock *et al.* [7], Gee *et al*. [6], and Nakamura and Takeuchi [5].

$$R_0 = \frac{ka^2}{2} \tag{3.1}$$

Frequency	Rayleigh Distance
1 kHz	0.59 cm
2 kHz	1.18 cm
10 kHz	5.9 cm
50 kHz	29.5 cm
100 kHz	59.09 cm

Table 3.1 Rayleigh Distances at given frequencies

3.2 Amplitude Comparison

A comparison of the radiated waveform at a single location with increasing initial pressure amplitudes will now be discussed. A 1 kHz pulse was propagated through the pipe at peak pressures of 225 Pa, 774 Pa, and 1200 Pa. Radiated waveforms were recorded on axis with the pipe ($\theta = 0°$) at a distance R = 2.54 cm and are shown in Fig 3.4 (a,b,c) respectfully. In Fig. 3.4(a), the radiated wave shows slight steepening from the incident waveform. Large losses also occur in peak amplitude, with the radiated waveform experiencing nearly a 50% loss. The initial waveform for Fig. 3.4(b) had a peak pressure of 774 Pa, a great increase from Fig. 3.4(a). The radiated waveform shows sharper peaks, which have narrowed in width when compared to Fig. 3.4 (a). The positive amplitude peak width is reduced from approximately 0.5 ms to 0.25 ms, with a peak pressure of 732 Pa, nearly equivalent with the initial peak pressure.

Continuing this trend, the radiated pulse from the initial 1200 Pa waveform is very distorted as it passes through the aperture. As seen in Figure 3.4 (c) the initial jump in pressure is extremely rapid with the waveform similar to those seen by Nakumura and Takeuchi [5]. Peak pressure has now exceeded that of the initial waveform at 1526 Pa.

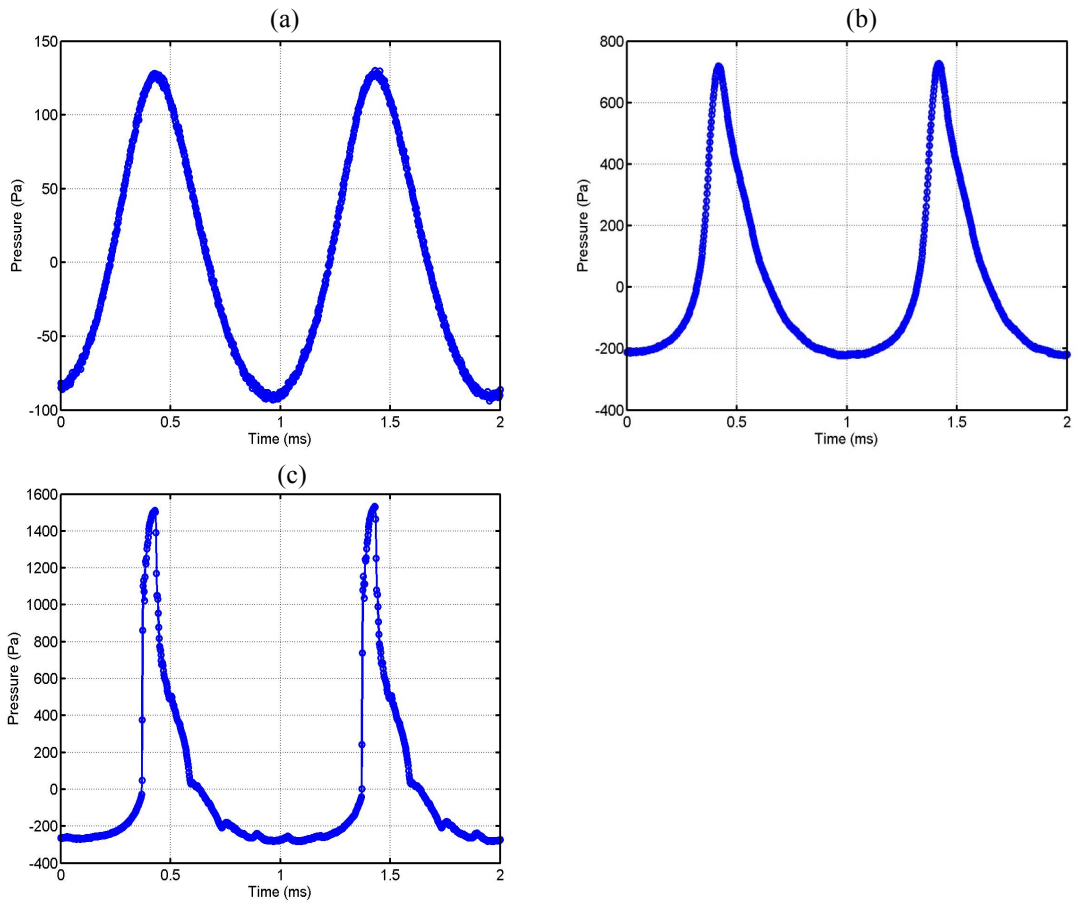

Figure 3.4 Radiated pressure waveforms measured at z=2.54 cm for 1 kHz sinusoid initial pulses with peak pressures of (a) 225 Pa, (b) 774 Pa, and (c) 1200 Pa.

These results are qualitatively expected when one considers both shock formation distance as well as the linearized momentum equation. For example, a doubling in initial peak amplitude reduces the shock formation distance by half. Due to the length of pipe remaining constant a more developed shock wave will be present at the end of the pipe. This creates a larger particle acceleration therefore increasing the distortion of the radiated waveform. At very high amplitudes the radiated waveform exceeds the initial wave's peak pressure. This is due to very large accelerations causing steep derivatives to occur as the shock formation distance decreases.

3.3 On-Axis vs. Off-Axis

A comparison will be made of the radiated waveforms on-axis with increasing R with $\theta = 0°$, followed by an increase in R as $\theta = 90°$. Peak pressures and positive peak widths will be discussed as they relate to these geometries.

3.3.1 On- Axis

Initial amplitude is now held constant at a 1200 Pa, and the 1 kHz sine wave is propagated through the pipe. On–axis positions of 0 cm, 2.54 cm, 12.7 cm, 25.4 cm are compared in Fig. 3.5(a-d), with R increasing in each successive plot. Figure 3.5(a) represents the pressure waveform right at the piston face and demonstrating the shape of the derivative as previously discussed. As r is held at 0 and z increases several characteristics are noticed.

First the full width half maximum (FWHM) of the peaks becomes increasingly narrow. A smaller timescale view is shown in Figure 3.6 of a single peak measured at 25.4 cm from the piston face, where the FWHM is only four samples in duration. This equates to a pulse width of 8 μs, which is incredibly small. This narrowing is explained in theory by the work done by Stepanishen [11]. He presents the idea that a radiated waveform from a pipe will be dependent on differences in arrival times from waves emanating from different locations on the pipe's aperture. As a sound wave exits a pipe, there are many radiation locations, starting from the center of the pipe and moving outward until the pipe edge. These waves at the boundary of the pipe are known as edge waves and dictate the radiated waveforms width. A large difference in arrival time from the center of the pipe and the edges of the pipe create wider waveforms. Utilizing

Pythagorean's theorum $R' = \sqrt{r^2 + R^2}$. As R increases and r is held constant the path length difference between R and R' becomes smaller, resulting in similar arrival times at the measured location. This creates the extremely narrow pulses seen in Fig. 3.6.

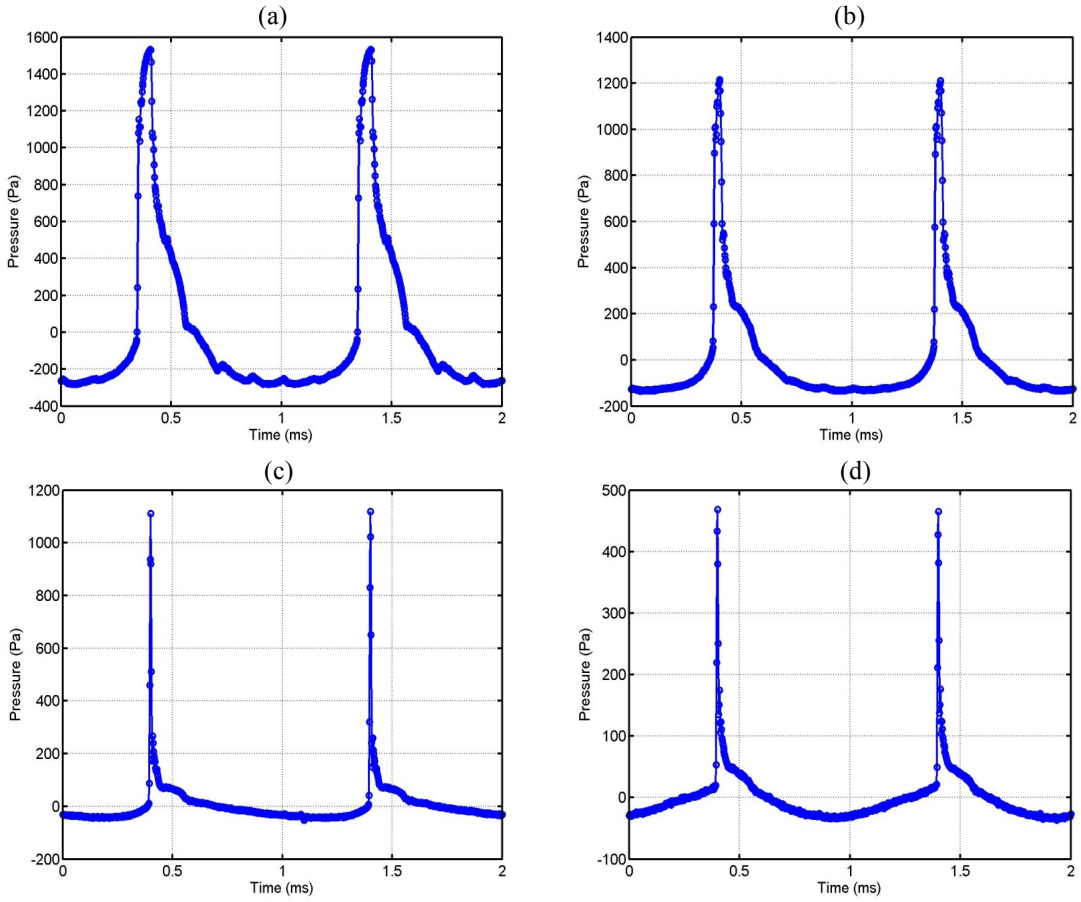

Figure 3.5 Pressure waveforms for a 1 kHz sinusoid initial pulse measured on-axis at (a) 0 cm, (b) 2.54 cm, (c) 12.7 cm, (d) 25.4 cm from the baffle. Initial peak pressure for 1 kHz was 1200 Pa

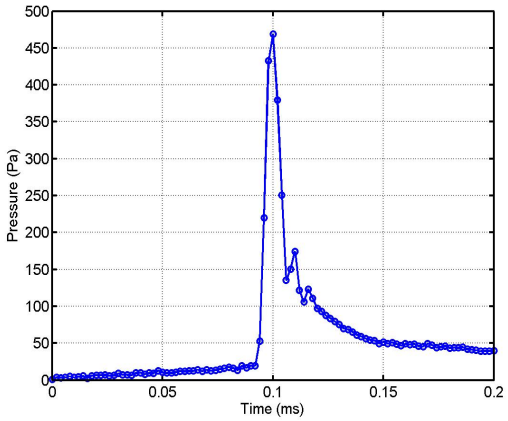

Figure 3.6 Pressure waveforms for a 1 kHz sinusoid initial pulse measured on-axis at 25.4 cm from the baffle. Initial peak pressure for 1 kHz was 1200 Pa

A second characteristic change that occurs is a reduction in peak amplitude as R increases. This is to be expected in linear piston theory due to geometric spreading. Geometric spreading predicts there to be a $\frac{1}{R}$ decrease in peak pressure as a wave propagates away from the source in the far field. Near field linear piston theory predicts a series of peaks and sharp troughs as the measurement location approaches R_0 [10]. However, the type of spreading recorded does not appear to match near field or far field linear piston theory, for overall peak amplitude or individual frequency amplitude, but rather is closer to cylindrical spreading. If Fig. 3.5 (b) is compared with Fig.3.5 (c), R increases by approximately a factor of five. Maximum amplitude does not respond with by decreasing by a factor of five. Spherical spreading would predict a drop from 1200 Pa to approximately 250 Pa, yet at 12.7 cm a peak pressure of 1100 Pa remains. Perhaps an easier comparison can be made between 12.7 and 25.4 cm. Spherical spreading predicts a drop from 1100 Pa to 550 Pa yet in this case the drop is actually greater with a peak value of 450 Pa at 25.4 cm. The only way this can be explained is due to nonlinearities

occurring or measurement error. As multiple tests were conducted with similar results a conclusion must be made that there are indeed nonlinear effects taking place.

3.3.2 Off-Axis

In contrast to an increasing R value on-axis, an off-axis investigation results in different characteristics. Figures 3.7 (a-d) show a radiated pulse measured at increasing R distances along the baffle ($\theta = 90°$). Unlike on-axis measurements once the microphone placement exceeds the pipe radius there is little change in the positive amplitude peak width at any value of R. Figure 3.7 (a) shows some narrowing due to edge waves arriving later than the center wave. Beyond the pipe boundary however, as Fig. 3.7(b,c,d) relates, the maximum difference in arrival times remains constant between propagation distances R' and R''. It is therefore possible to conclude that the maximum peak width at a given initial amplitude is defined by the diameter of the pipe.

Peak amplitude also behaves differently off-axis, resulting more closely in a spherical spreading trend. The doubling in distance from Figure 3.7 (c) to Figure 3.7 (d) results in a drop in amplitude from 150 Pa to 82 Pa a factor of just over one half. When compared to the drop to 75 Pa expected from linear piston theory for a 1 kHz signal, off-axis results seem to spread far more spherically. The 7 Pa difference can be explained with spectra and the directivity of a baffled piston (see sec. 3.6).

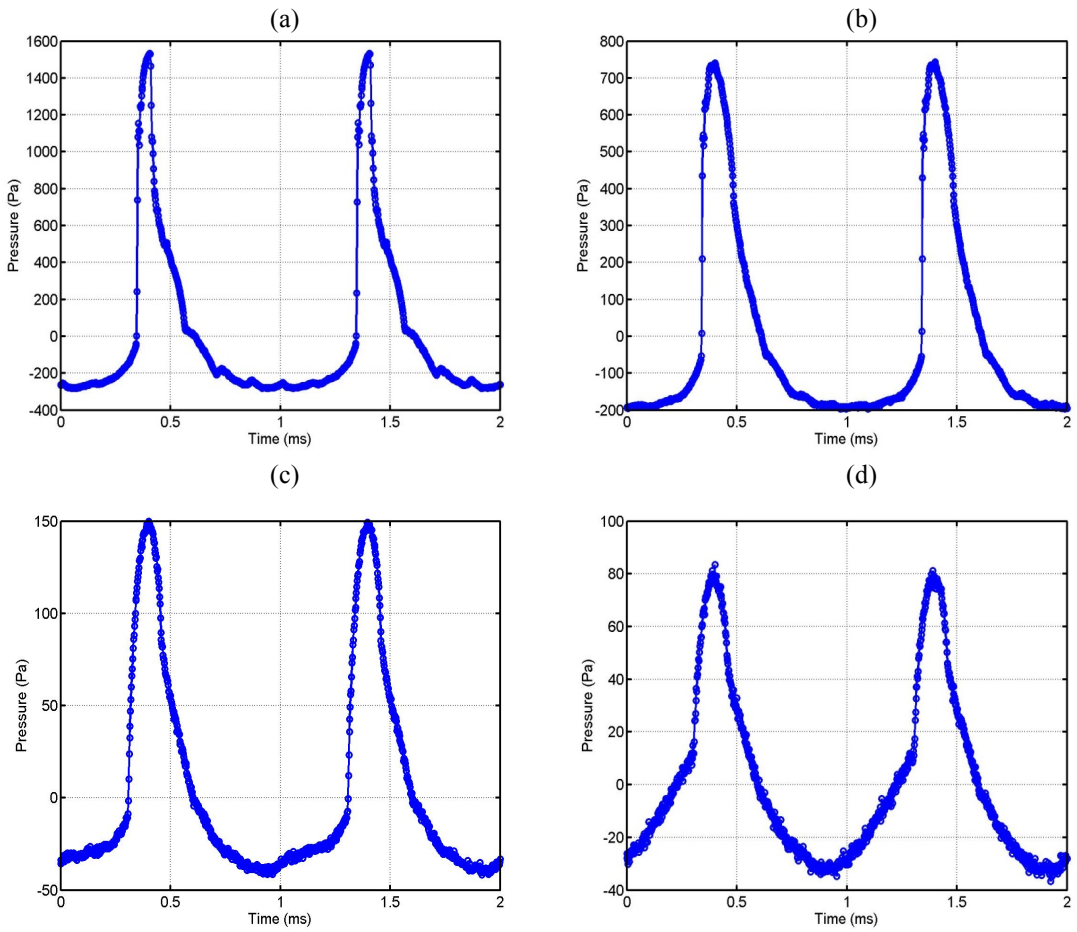

Figure 3.7 Pressure waveforms for a 1 kHz sinusoid initial pulse measured off-axis at (a) 0 cm, (b) 2.54 cm, (c) 12.7 cm, (d) 25.4 cm from center of the pipe. Initial peak pressure for 1 kHz was 1200 Pa

3.4 Angular Comparison

In addition to the comparisons discussed, an angular study was also conducted. In this thesis, only a radius R of 12.4 cm will be presented for direct angular comparison. Figure 3.8 (a-d) displays the results of the pressure waveform measured at $\theta = 0°$, $30°$, $60°$, and $90°$ respectively. In Fig. 3.8 (a) the peak amplitude is 1116 Pa and has a very narrow peak

width, approximately 1 μs FWHM. As the measurement location shifts by just 30° (Fig. 3.8 (b)) the change is very noticeable.

At 30° peak amplitude is greatly reduced, in this case it has dropped to 1/5 of the on-axis value. Additionally the peak width has increased to approximately 56 μs. Peak amplitude decrease and FWHM increase continues through 60°. Figure 3.8(c,d) demonstrate that beyond 60° there is little change in either peak amplitude or width. This lack of change in wave shape can be explained by simple geometry. With R=12.4 cm, the differences in path lengths from the edge waves in Fig 3.8 (c) at 60° is very close to those at 90° in Fig 3.8 (d). This results in very little shift in the waveform's shape between the two locations. If R was increased to be much greater, it is expected that there would be a more significant difference beyond 60° due to a larger difference in path lengths R' and R''.

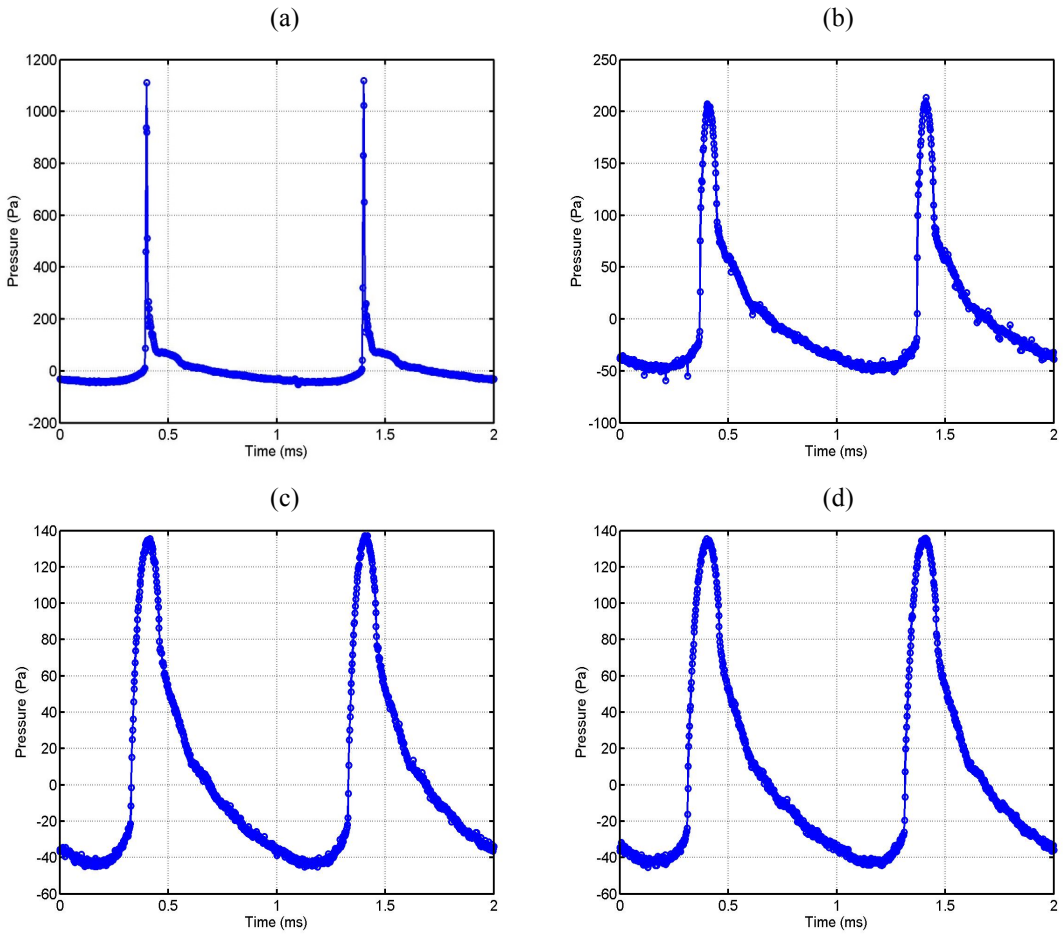

Figure 3.8 Pressure waveforms for a 1 kHz sinusoid initial pulse measured at R= 12.4 cm at (a) 0°, (b) 30°, (c) 60°, (d) 90°. Initial peak pressure for the 1 kHz sinusoid was 1200 Pa

3.5 Frequency Comparison

A similar test was done to that in sec. 3.4 with a 2 kHz sinusoidal waveform with peak pressure of 1015 Pa, as the incident signal. The results can be seen in Fig. 3.9 (a-d) in direct comparison to radiated waveforms of the 1 kHz case at the same locations. When comparing the two frequencies' radiated waveforms, it is apparent that frequency has little to no effect on the positive pressure FWHM. At every angle, the FWHM of the 2 kHz radiated wave is the same as the 1 kHz case. There are double the number of peaks in the same period of time as expected with the doubling in frequency but the waveform's shape is unaffected. This leads to the conclusion that high amplitude radiation from a baffled piston is geometry based and frequency independent beyond the baffle in regards to FWHM.

A less obvious result is that of radiated peak amplitude. The peak amplitudes of every 2 kHz data set is lower than the 1 kHz counterpart. As the initial waveform at 2 kHz has lower peak amplitude this might be expected. However, when doubling the frequency of a signal this also reduces the shock formation distance to half of what it was for a 1 kHz signal. This being the case, shock waves for the 2 kHz case should develop faster and have a higher σ value for the same pipe length (Equation 1.1). The result should theoretically place the radiated peak amplitudes significantly higher than the 1 kHz case. This is not the measured result as seen in Figure 3.9. The solution in part presents itself in the spectral information of the radiated peaks. Figure 3.10 shows the spectra of on-axis radiated pulses of both the 1 and 2 kHz signals. The spectra are very similar as expected, however the 2 kHz case lacks half of the higher

harmonic frequencies that the 1 kHz signal contains, theoretically reducing the energy of the wave form by half resulting in peak amplitudes similar to those at 1 kHz.

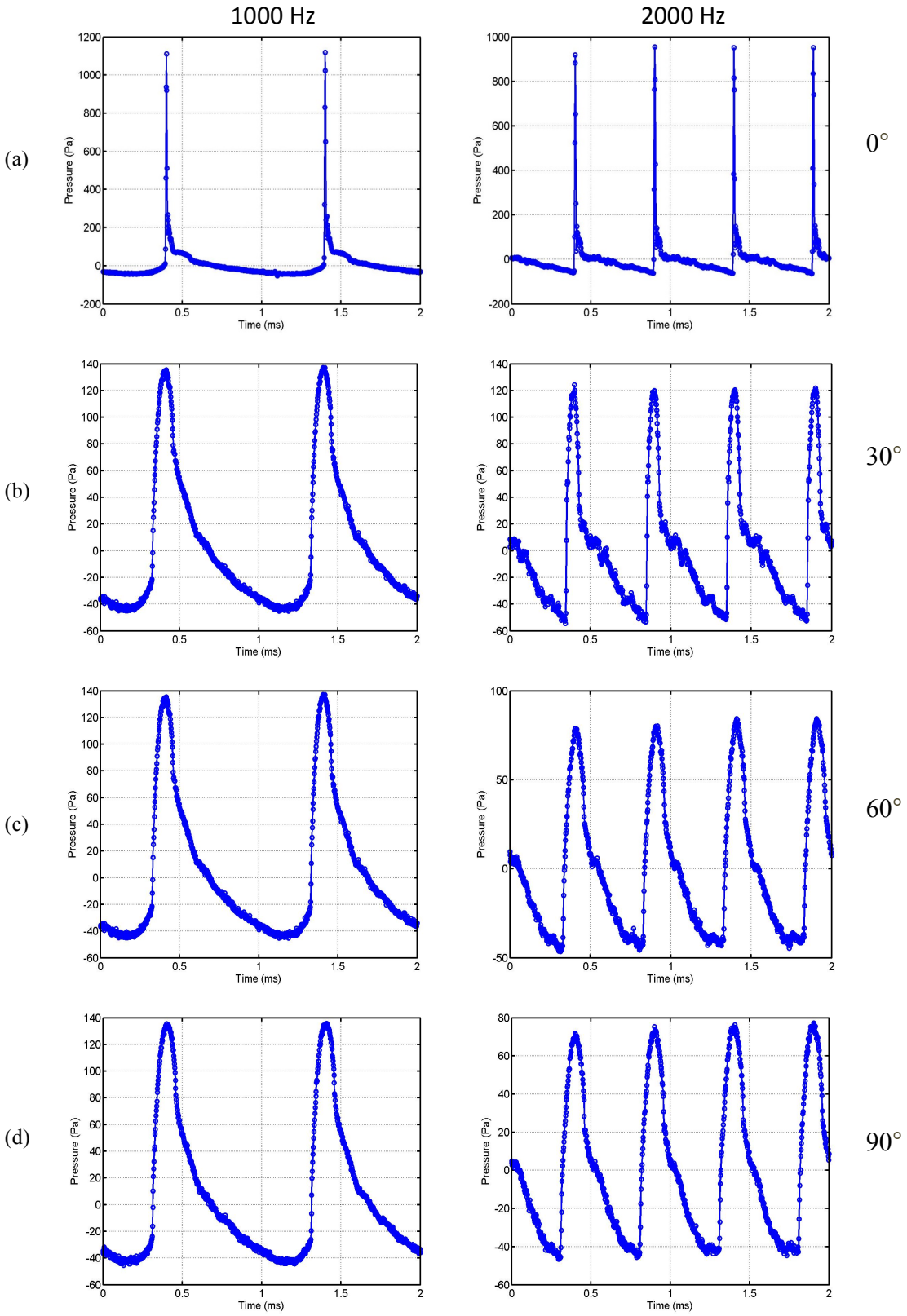

Figure 3.9 Pressure waveforms for a 1 kHz and 2 kHz sinusoid initial pulse inside tube measured at R= 12.4 cm at a) 0°, b) 30°, c) 60°, d) 90°. Initial peak pressure for 1 kHz was 1200 Pa and for 2 kHz was 1015 Pa

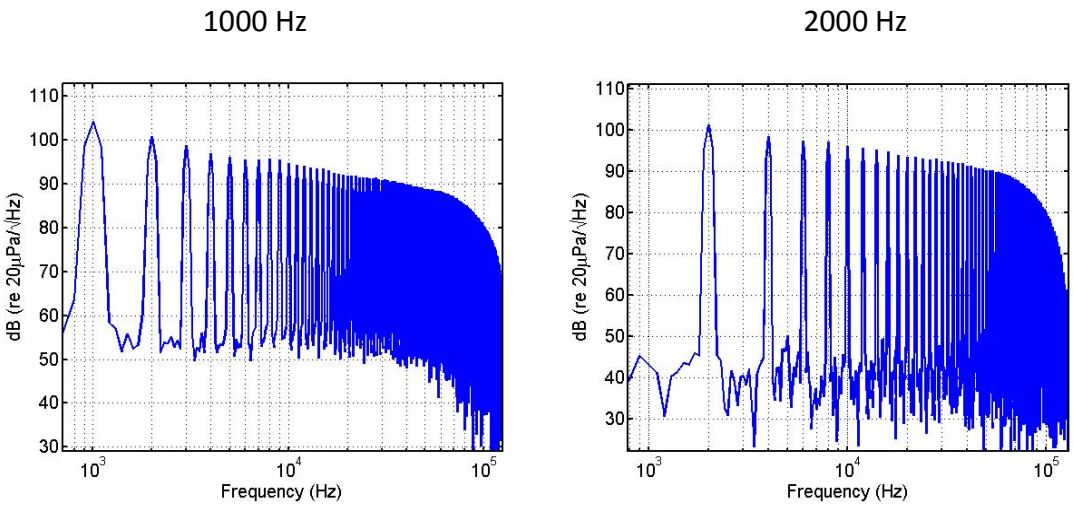

Figure 3.10 Spectrum of radiated waveforms for 1 kHz and 2 kHz pulses at R = 12.7 cm on-axis. Initial peak pressure for 1 kHz was 1200 Pa and for 2 kHz was 1015 Pa

3.6 Peak Pressures

Figure 3.11 presents a contour plot of the radiated wave's peak pressures over area for 1 kHz data. The x-axis represents increasing on-axis distance away from the center of the pipe. The y-axis similarly represents the off-axis distance along the baffle increasing away from the center of the pipe. The contour lines and colors display peak pressure levels.

Due to the high amplitudes of the waveforms, higher frequency spectral content becomes more important, and, with a 500 kHz sampling frequency, frequencies up to 250 kHz are relevant. As frequency increases radiation patterns become more directional. In Fig. 3.12 the directivity patterns for a sinusoidal wave of multiple frequencies are shown. This results in contributions from high-amplitude harmonic content significantly

effecting peak pressure near 0°, while contributing significantly less at locations farther off axis.

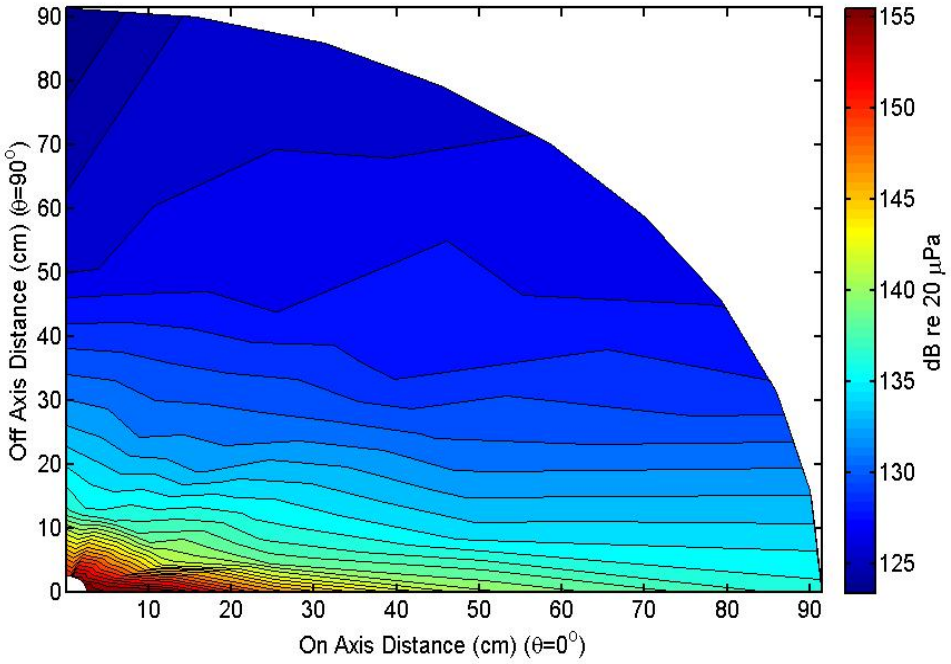

Figure 3.11. Peak amplitude of radiated waveforms of an initial 1 kHz sinusoidal pulse with an initial peak amplitude of 155.5 dB

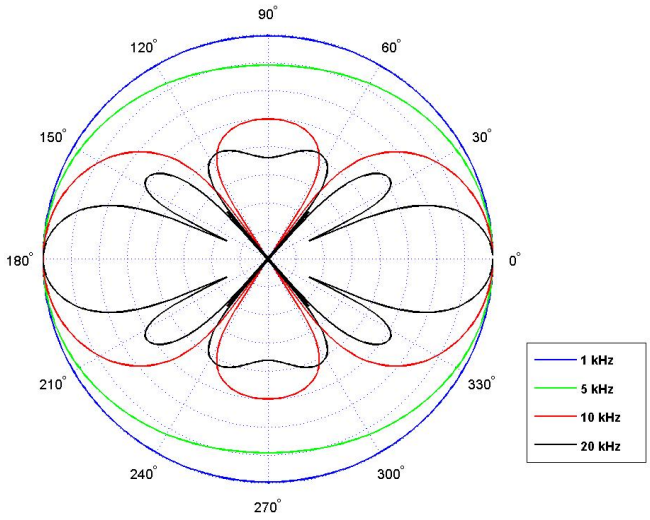

Figure 3.12. Directivity patterns of a baffled piston at four frequencies. The piston face radiates outward toward 0° with the baffle along the 90° axis.

Little has been discussed thus far about any evidence of nonlinear effects occurring as the radiated waveform propagates away from the pipe. The characteristics of the radiated wave can been explained by linear theory, yet with peak amplitudes over 150 dB in some regions, nonlinear behavior cannot be discounted. The peak pressure map from Fig 3.11 demonstrates the possibility that nonlinear effects are indeed occurring, as the on-axis peak pressure contour is examined the curve rolls off faster than linear piston theory suggests. As shown in Fig. 3.13, at 20 cm on-axis the maximum pressure is approximately 151 dB. At four times that distance, 80 cm, the pressure has been reduced to 137 dB. This equates to a 14 dB drop in pressure over two doublings in distance. Linear theory expects a 6 dB reduction per doubling in distance or in this case 12 dB for a quadrupling. Although not conclusive, it is probable that peak amplitude decreases faster than expected due to nonlinear effects.

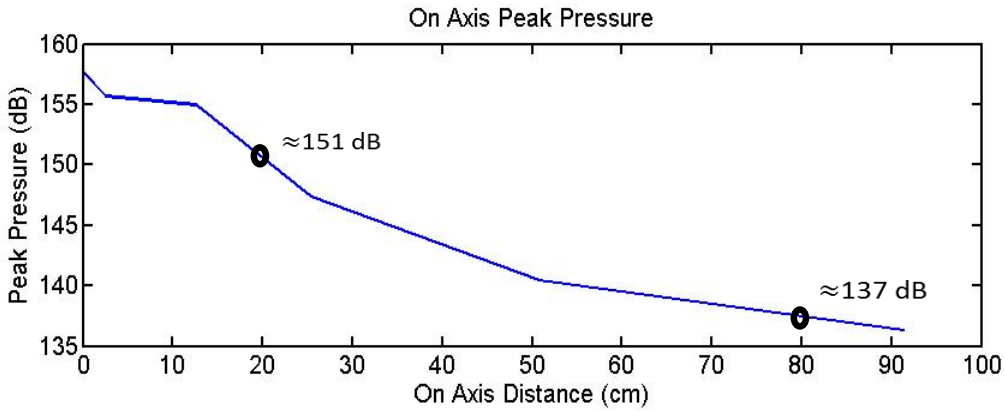

Figure 3.13 Peak pressures of radiated waveform measured on-axis of an initial 1 kHz sinusoidal pulse. Initial peak pressure was 155.5 dB.

Additionally when collected data is directly compared with far field baffled piston directivity in Fig 3.14 there are definite discrepancies. At R = 12.7 cm frequencies up to 10 kHz are categorized as far field and measured data should agree with linear piston theory. However, Fig. 3.14 shows definite discrepancies especially for the 5 kHz and 10 kHz frequencies. These differences may be a result of nonlinear behavior occurring, but whether this is the case or if the discrepancies can be attributed to signal processing error or some other reason is currently unknown. Further investigation will be required to explain these results.

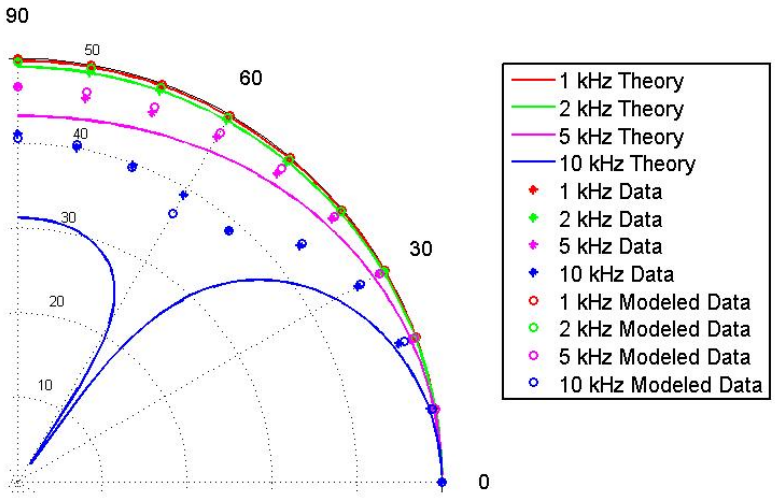

Figure 3.14 Baffled piston directivity plot for Linear theory (solid lines), Measured data (*), and Modeled data (o). Different frequencies are represented by colors: Red (1 kHz), Green (2 kHz), Magenta (5 kHz), Blue (10 kHz).

3.7 Noise

To ensure that the aforementioned radiation patterns were not dependent on a periodic signal, band-limited Gaussian noise was also propagated down the pipe. The signal was pulsed just as the sinusoidal signal, in short bursts with frequency limits of 0.9 – 1.6 kHz. Peak amplitude was not relevant as noise is rarely measured with peak amplitudes, however, maximum peaks were seen in the initial signal which are comparable to the 1 kHz, 1200 Pa signals previously used. Fig. 3.15 (a) demonstrates similar impulse like peaks being radiated at 12.7 cm on-axis to those of both 1 kHz and 2 kHz signals allowing a conclusion of signal invariance to the behavior of a radiated wave from a baffled pipe at high amplitude.

It is of some value to compare the spectra from a radiated noise signal (Fig. 3.15 (b)) to that of the radiated sinusoid waveform (Fig. 3.15 (d)). One expects a train of

perfect delta functions to have a spectrum with 0 dB/decade roll off, just as white Gaussian noise should have no roll off. The spectrum of a sawtooth wave has a roll off of approximately 20 dB/decade, which if radiated from a piston should create a perfect train of delta functions. The spectrum seen in Fig. 3.15 (d), rolls off at approximately 10 dB/decade, somewhere in between a sawtooth wave and a delta function train, demonstrating that the driving signal is not a perfect sawtooth but, due to the roll off being between 10 and 20 dB/decade, non-linear in nature. It should follow that as the shock formation distance is decreased the delta function like peaks seen in Figure 3.15 (c) would become more like a train perfect impulses. This would cause the roll off of the power spectrum to flatten out. Further investigation would be appropriate in order to investigate this theory.

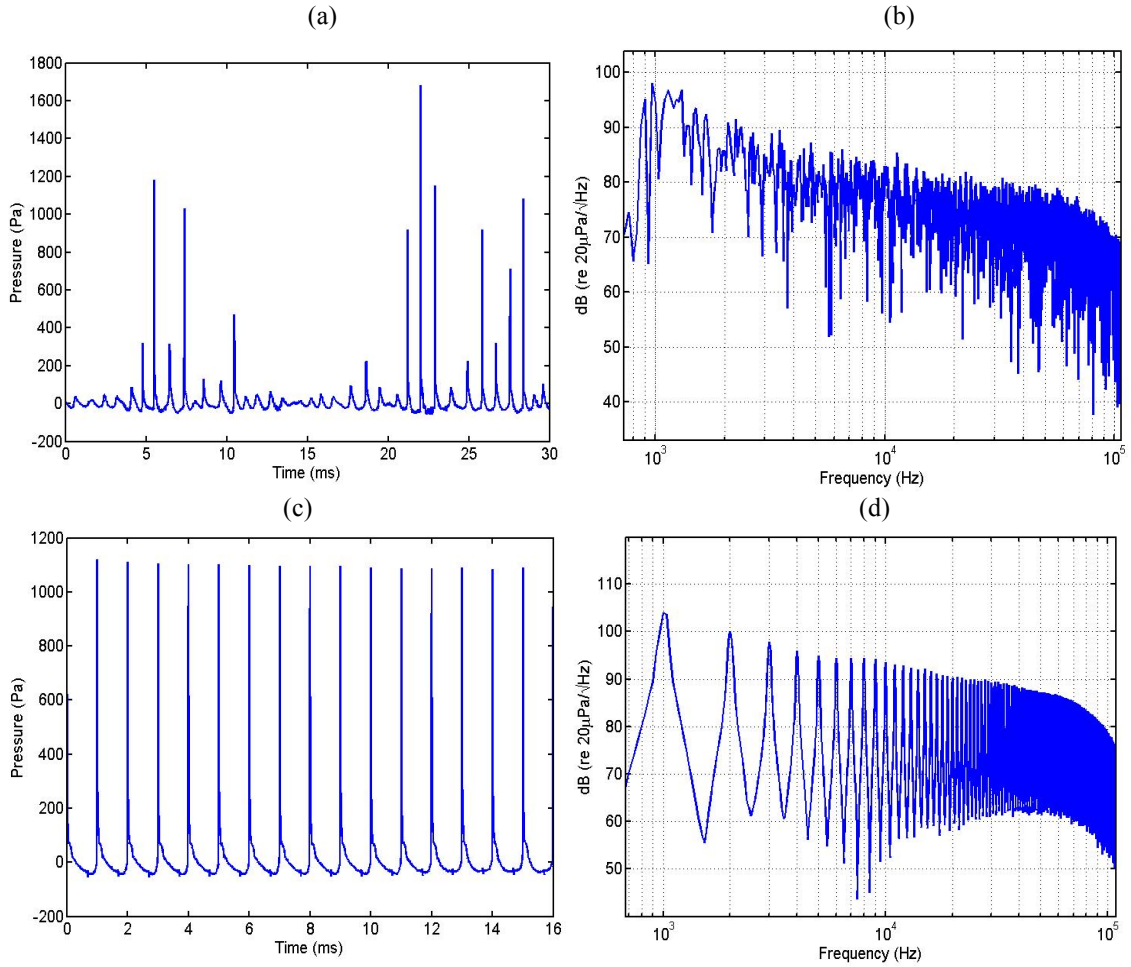

Figure 3.15 (a) Radiated waveform from a 0.9-1.6 kHz band limited Gaussian noise signal measured on-axis at R=12.7 cm. (b) The power spectrum of (a). (c) The pressure waveform from a 1 kHz pulse radiated as measured on-axis at R=12.7 cm. (d) the spectrum of (c).

Chapter 4

Analytical Model

4.1 Model Development

Blackstock *et al.* [8] predicted impulse-like waveforms produced by a baffled piston by applying the Greens' function to time-dependent pressures achieved from particle velocities at the pipe boundary. This work was stems from Stepanishen, however, the cross modes in the pipe and open-end reflections were not included in the model. Equations 4.1 through 4.4 are directly from the work done by Stepanishen and were used to build the model presented in this paper. [11]

$$P1(x,t) = \frac{\rho c}{\pi}\int_{R'}^{R''} \cos^{-1}\left[\frac{(c\tau)^2 - z^2 + r^2 - a^2}{\left(2r\sqrt{(c\tau)^2 - z^2}\right)}\right] v'\left(t - \frac{R''}{c}\right) d\tau \tag{4.1}$$

$$P_2(x,t) = \rho c[v\left(t - \frac{z}{c}\right) - v\left(t - \frac{R''}{c}\right)] \tag{4.2}$$

$$R' = \sqrt{z^2 + (a+r)^2} \tag{4.3}$$

$$R'' = \sqrt{z^2 + (a-r)^2} \tag{4.4}$$

A detailed analysis of the origins of these equations can be found by reading Stepanishen and will not be presently discussed. It is sufficient to state that if $r > a \;\; P = P_1(x,t)$ and if $r < a \;\; P = P_1(x,t) + P_2(x,t)$ [11] (eq. 4.1 & 4.2). This model incorporates Stepanishen's equations in addition to modeled radiation impedance. The initial waveform used for the model is the actual measured waveform from the microphone at 605 cm from the driver (Fig. 3.3 (c)). This is a deviation from Blackstock *et al.* [8] who used a perfect N-wave for their model. These changes were made in order to more accurately model the measured radiated waveform.

4.2 Data/Model Comparison

Comparisons are made from real collected data to that of the analytical model for three previously discussed results including: on-axis, off-axis and angular comparisons. They are shown in figures 4.1, 4.2, and 4.3 respectively. Results shown in red are modeled and those in blue are collected data.

It is difficult to make many quantitative comparisons between model and data, as there are many areas where the model breaks down. Negative pressure values tend to be very inaccurately modeled possibly due to numerical artifacts and other undetermined effects. Also peak amplitudes do not compare accurately, this is most likely due to the lack of directivity built into the model as well as its dependence on linear theory. When the peak amplitudes are normalized data and model closely match at most frequencies as shown in Fig. 3.15. What the model does well in most cases is to predict the general positive waveform shape as well as width of the positive pressure of the waveform. This is done particularly well in the on-axis case where the integrated portion of the model (eq.

4.1) evaluates to a constant therefore reducing the amount of artifacts present. The obvious discrepancies between the model, measured data and theory, help to support the idea of non-linear effects occurring during radiation.

It should be noted that upon completion of this work and gaining Dr. Blackstock's opinion on these results, he concluded that the current model is too simple and needs to be modified to incorporate other phenomenon. This will be for future work and the possible incorporated changes that could occur will not be discussed here.

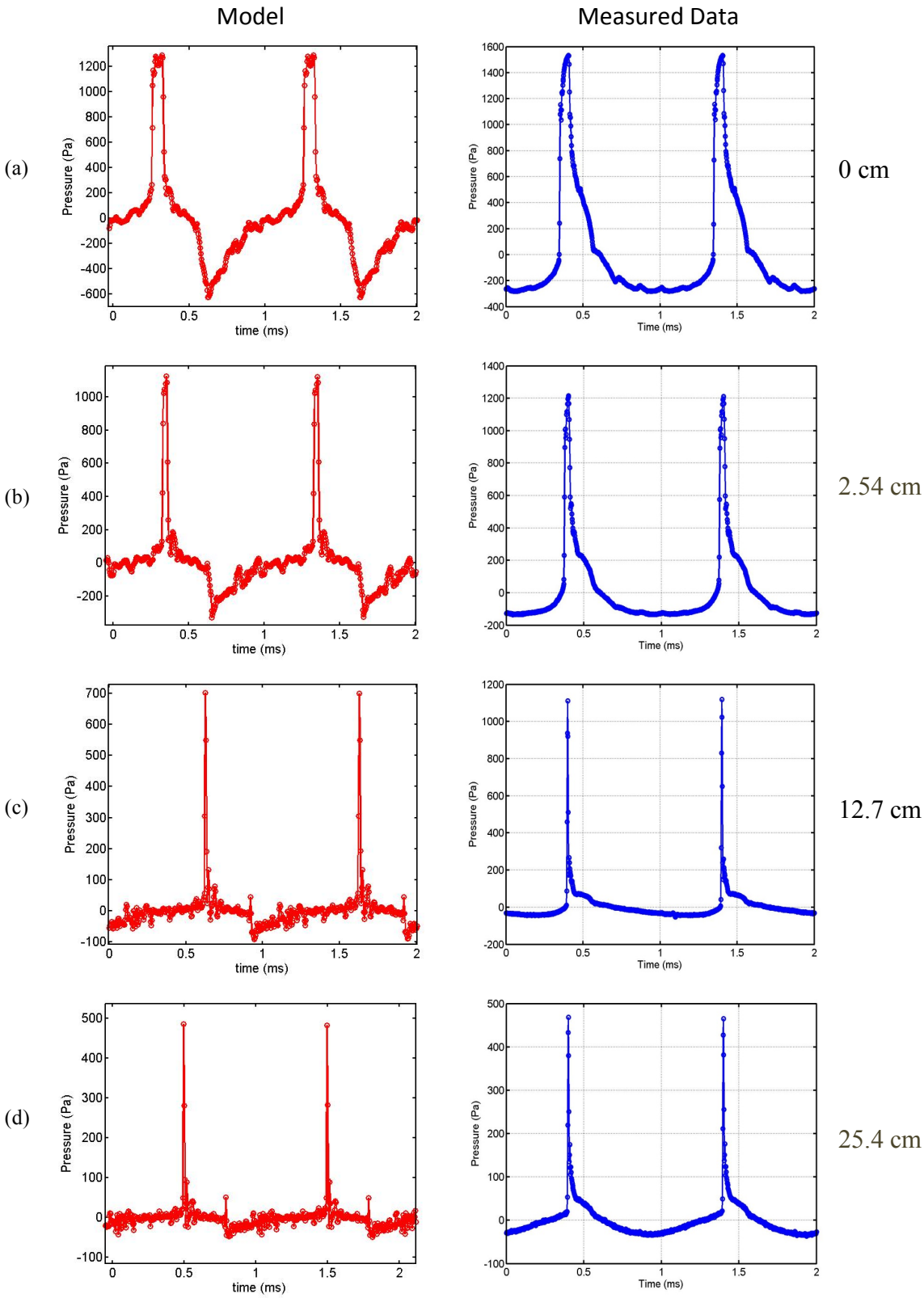

Figure 4.1 Comparison of model (red) and measured data (blue) for radiated waveforms on-axis at a) 0 cm, b) 2.54 cm, c) 12.7 cm, d) 25.4 cm from the baffle. Initial peak pressure for 1 kHz signal was 1200 Pa.

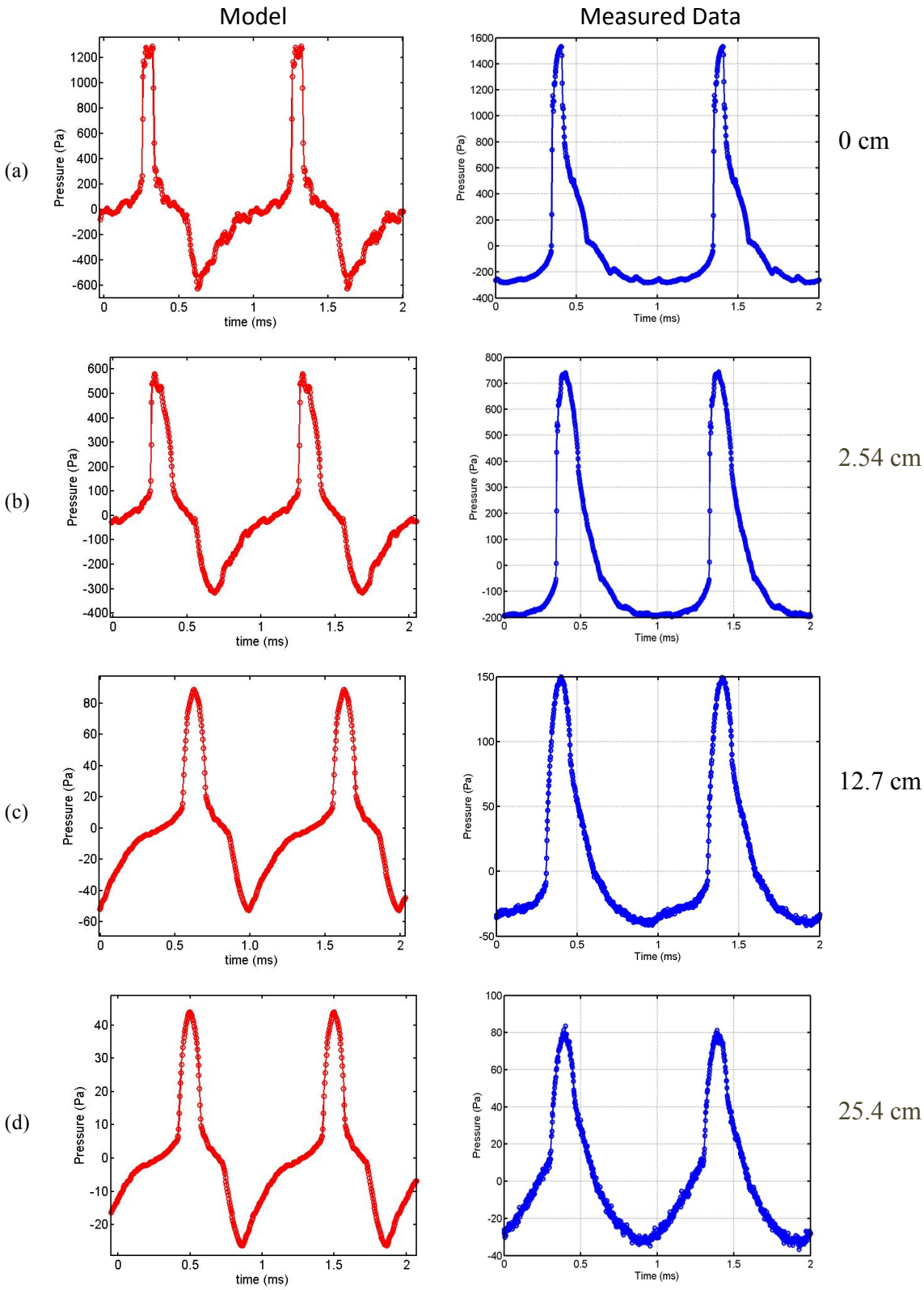

Figure 4.2 Comparison of model (red) and measured data (blue) for radiated waveforms off-axis at a) 0 cm, b) 2.54 cm, c) 12.7 cm., d) 25.4 cm from the baffle. Initial peak pressure for 1 kHz signal was 1200 Pa

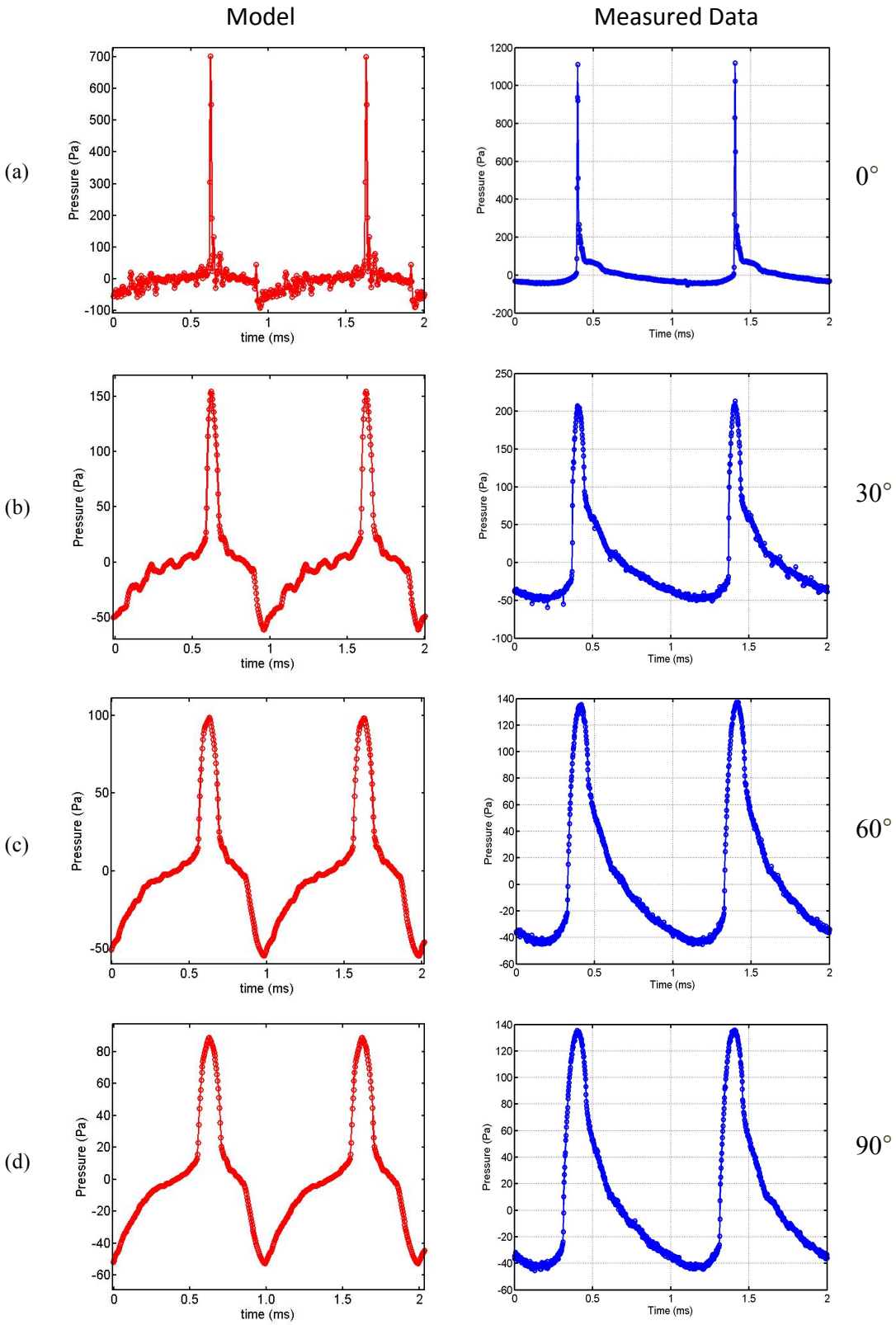

Figure 4.3 Comparison of model (red) and measured data (blue) for radiated waveforms off-axis at R= 12.4 cm at a) 0°, b) 30°, c) 60°, d) 90°. Initial peak pressure for 1 kHz signal was 1200 Pa

Chapter 5

Conclusion

An in depth study has been conducted on the radiation of finite amplitude waves from a baffled pipe. Work done by Blackstock *et al.* [8] has been expanded and a more complete study has taken place, including on and off axis, angular, frequency, peak amplitude, and noise comparisons. A modified analytical model has also been created and compares accurately in some respects to existing data. It has been shown that the radiated waveform's shape is dependent on both off-axis and on-axis distances, and is dictated by arrival times from the center and edges of the pipe. As on-axis distance increases the radiated waveform narrows and becomes more impulse like. Additionally the patterns seen in radiated waveforms are signal type independent, but rather depend on pipe diameter and shock formation distance.

Many effects of the radiated wave form can be explained under linear theory, however there are several things including peak amplitude roll off and lack of accuracy with the linear directivity model which provide basis for arguing that non-linear effects are occurring. In the future more work can be done to improve the current model as well

as to investigate the possibility of thermal or other effects that could be contributing to the discrepancies with linear theory.

Bibliography

[1] A. Hirschberg, J. Gilbert, R. Msallam, and A. P. J. Wijnands, "Shock waves in trombones," J. Acoust. Soc. Am. **99**, 1754 - 1758 (1996).

[2] M. W. Thompson and W. J. Strong, "Inclusion of wave steepening in a frequency-domain model of trombone sound production," J. Acoust. Soc. Am. **110**, 556-562 (2001).

[3] N. Sekine, S. Matsumura, K. Aoki, and K. Takayama, "Generation and propagation of shock waves in the exhaust pipe of a 4 cycle automobile engine", AIP Conf. Proc. 208, 671 (1990).

[4] H. D. Kim and T. Setoguchi, "Study of the discharge of weak shocks from an open end of a duct," J. Sound Vib. **226**, 1011-1028 (1999).

[5] A. Nakamura and R.Takeuchi, "Reflection and transmission of acoustic shock wave at a boundary," Acustica **26**, 42-50 (1972).

[6] K. L. Gee, V. W. Sparrow, M. M. James, J. M. Downing, and C. M. Hobbs, "Measurement and prediction of nonlinearity in outdoor propagation of periodic signals." J. Acoust. Soc. Am. **120**, 2491 - 2499 (2006).

[7] D. T. Blackstock , W. M. Wright, and J. R. Kuhn, "Radiation of sawtooth waves from the open end of a pipe" (Unpublished manuscript).

[8] J. R. Kuhn, D. T. Blackstock, and W. M. Wright, "Radiation of sawtooth waves from the open end of a pipe," J. Acoust. Soc. Am. **63**(S1), S84 (1978).

[9] D. T. Blackstock, M. F. Hamilton., and A. D. Pierce, "Progressive Waves in Lossless and Lossy Fluids", in *Nonlinear Acoustics*, edited by M. F. Hamilton and D. T. Blackstock (Academic Press, 1998), pp. 65-150.

[10] D. T. Blackstock, "Radiation from a Baffled Piston", in *fundamentals of physical acoustics*, (*A Wiley-Interscience publication*, 2000), pp. 440-471.

[11] P. R. Stepanishen, "Transient radiation from pistons in an infinite planar baffle," J. Acoust. Soc. Am. **49**, 1629-1638 (1971).

[12] J. Y. Chung and D. A. Blaser, "Transfer function method of measuring in-duct acoustic properties. I. Theory," J. Acoust. Soc. Am. **68**, 907 – 913 (1980).